

Faceting Transformations of the Stepped Pt(001) Surface

G. M. Watson and Doon Gibbs

Physics Department, Brookhaven National Laboratory, Upton, New York 11973-5000

D. M. Zehner

Solid State Division, Oak Ridge National Laboratory, Oak Ridge, Tennessee 37831-6057

Mirang Yoon and S. G. J. Mochrie

Department of Physics, Massachusetts Institute of Technology, Cambridge, Massachusetts 02139-4307

(Received 18 August 1993)

We describe x-ray scattering studies of the structure and morphology of a stepped Pt(001) surface between 300 and 1850 K. Two distinct faceting transformations are observed. Above 1820 K, we find an unreconstructed, stepped surface. Between 1820 and 1620 K, there is coexistence among hexagonally reconstructed, step-free domains and unreconstructed, stepped domains. The tilt angle of the unreconstructed domains exhibits a one-half power-law dependence on reduced temperature. At 1620 K, there is a second morphological transformation at which the unreconstructed domains are replaced by *magic vicinals*.

PACS numbers: 68.35.Rh, 61.10.Lx, 64.70.Kb

Equilibrium faceting is a remarkable phenomenon in which a crystal surface increases its area in order to decrease its free energy. It is accomplished through the rearrangement of surface steps so that their distribution across the surface is no longer uniform. Instead, the surface separates into regions of high and low step density. Our present understanding of faceting is based on a description of the surface free energy in which the surface orientation is a key thermodynamic variable. Thus, a *faceting transformation* is an example of thermodynamic phase separation in which a surface phase of uniform orientation is replaced by coexistence among phases with different orientations and separated by sharp edges.

Faceting may occur near a surface phase transformation when two phases exist with different step energies [1-6]. In particular, Phaneuf and Williams have shown that certain stepped Si(111) surfaces undergo faceting at the (7×7) to (1×1) transformation [3,4,6]. In this case, the free energy of a step on the (7×7) surface is greater than that on the unreconstructed surface. Below the (7×7) to (1×1) transformation temperature, the free energy of the macroscopically miscut surface is lowered by phase separation into unreconstructed domains of high step density in coexistence with step-free facets of (7×7) reconstruction.

A second avenue to faceting involves the presence of steps on a reconstructed surface. Here, the surface free energy may have a local minimum when the steps are commensurate or nearly commensurate with the reconstruction, again leading to the possibility of faceting. These special orientations are called *magic vicinals* [7], and to our knowledge have not previously been observed.

In this paper, we summarize the results of an x-ray scattering study of the structure and morphology of a stepped Pt(001) surface between 300 and 1850 K (the bulk melting temperature is 2040 K). Earlier studies of

nominally step-free Pt(001) surfaces [8-10] have established a fascinating phase behavior, including a first-order transformation from a rough to a hexagonally reconstructed structure at about 1820 K and rotational transformations of the incommensurate, hexagonal overlayer below 1685 K. Our motivation in the present experiments was to explore the effects of steps on these transformations, particularly in light of the general perspectives of faceting noted above.

In the experiments reported here, the surface normal of the sample was deliberately miscut by 1.4° away from the (001) direction and towards the (110) direction, which corresponds to an average monatomic step separation of approximately 30 near-neighbor distances. For temperatures above $T_0=1820$ K, we find that the surface reflectivity is aligned to the direction of the macroscopic miscut. Its line shape is diffuse, and suggests that the miscut surface is rough, as was found for (001)-oriented Pt surfaces at these temperatures [8-10]. Below 1820 K, there is a faceting transformation, which leads to coexistence among hexagonally reconstructed, step-free domains, called facets, aligned to the (001) direction [8,9] and stepped, unreconstructed domains [10]. Between 1820 and 1620 K, the phase behavior of the (001) facets is similar to that of the Pt(001) surface [8,9,11]. On the stepped domains, the surface normal is tilted at an angle α to the (001) direction [see inset (b), Fig. 1]. Remarkably, our data show that α follows a one-half power-law dependence on reduced temperature [$t=(T_0-T)/T_0$]. This implies that the free energy of a rough, solid surface varies quadratically with misorientation, consistent with simple theoretical ideas.

At 1620 K, there is a second faceting transformation at which the rough domains disappear. Instead, the surface is populated by two new domain types with ordered step distributions, in addition to the step-free, hexagonally

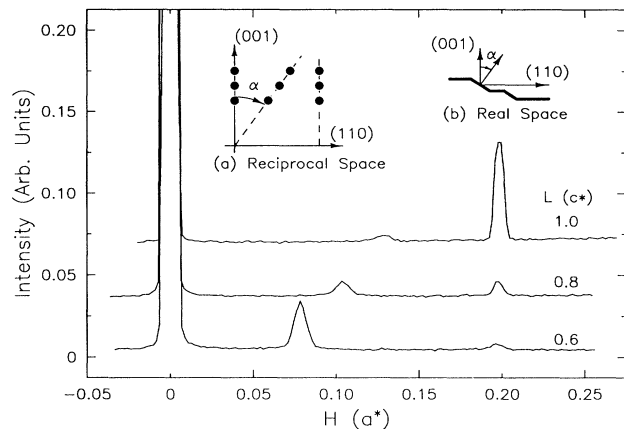


FIG. 1 X-ray scans along the $(HH0)$ direction for three values of L at 1727 K. Insets: (a) locations in reciprocal space of the observed peaks and (b) schematic real-space model showing (001) facets and stepped domains. The stepped domains are tilted at an angle α to the (001) direction.

reconstructed (001) facets. The terraces of the stepped domains are reconstructed to form a buckled and rotated hexagonal structure. Surface buckling refers to the sinusoidal displacement of atoms along the surface normal direction, and is a defining characteristic of the close-packed, hexagonal reconstructions of Pt and Au (001) surfaces [8,9]. Our data show that the troughs and crests of the surface buckling are parallel to the step edges. This suggests that the rotation angle of the hexagonally reconstructed, stepped domains may be determined by the step orientation, consistent with the symmetry principle of Grey and Bohr [12]. Finally, for temperatures below 1500 K, the step wave vector locks to the buckling wave vector with a periodicity 4 times smaller than the terrace width. This corresponds to the formation of a commensurate magic vicinal. A complete account of our results and analysis is presented in Ref. [11].

The experiments were performed on beam lines X20A and X22C at the National Synchrotron Light Source using UHV instruments which have been described previously [8,9,13]. The sample mosaic was 0.01° full width at half maximum (FWHM). High-resolution experiments were performed in a glancing incidence geometry at a fixed surface normal wave vector $L=0.05$ and using a Ge (111) analyzer. The radial resolution obtained at the (002) reflection was 0.0011 \AA^{-1} FWHM with an incident photon energy of 8 keV. Otherwise, slits defined both the illuminated sample area and the spectrometer resolution. At $L=0.8$ on the specular rod, this gave a resolution width of 0.10 \AA^{-1} along the (001) direction and widths of approximately 0.01 \AA^{-1} along the $(1\bar{1}0)$ and (110) directions.

Representative scans obtained near the condition for specular reflection at 1727 K are shown in Fig. 1. These scans were taken along the (110) direction (which corre-

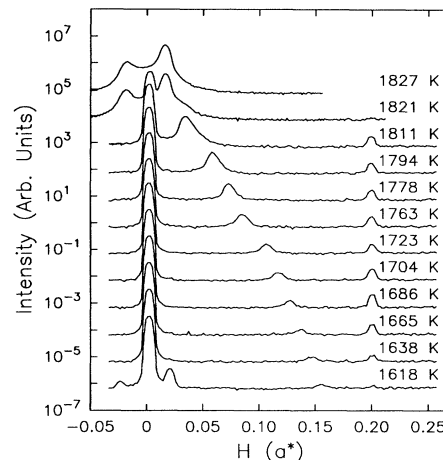


FIG. 2. Scans along the $(HH0)$ direction at $L=0.89$ versus temperature. The truncation rod passing through the (002) bulk Bragg reflection shifts to larger negative H with decreasing temperature and is not shown in the figure.

sponds to the azimuthal direction of the macroscopic miscut) for three different values of L . The two peaks at $H=0$ and 0.2 are independent of L and originate from facets aligned to the (001) direction. Specifically, the peak at $H=0$ corresponds to the specular reflectivity, while the peak at $H=0.2$ corresponds to the buckling wave vector of the hexagonal reconstruction. In contrast, the position of the third peak in Fig. 1 shifts to larger H as L increases. As shown in Fig. 1, inset (a), this rod intersects the origin of reciprocal space and is tilted away from the (001) direction by an angle $\alpha = \tan^{-1}(\sqrt{2}H/L) = 10.5^\circ$. This rod corresponds to the specular reflectivity of the unreconstructed, stepped domains. Thus, at 1727 K, the scattering from stepped Pt (001) consists of two sets of rods from two distinct phases with different surface normal directions [see Fig. 1, inset (b)].

Figure 2 shows scans taken along the (110) direction at fixed $L=0.8$ for temperatures decreasing from 1827 K. At the highest temperature, only two peaks are observed, each displaced from $H=0$. Characterization of their L dependence has shown that they correspond to rods oriented at an angle of 1.4° to the (001) direction, and along the direction of the macroscopic miscut. In fact, the peak at positive H corresponds to the specular rod, while that at negative H corresponds to the truncation rod emanating from the (002) bulk Bragg reflection. It follows that at this temperature the surface is comprised of a single orientation; that is, it lies in a one-phase region of the temperature-orientation phase diagram, in contrast to the situation at 1727 K. The broad line shape of the specular rod suggests that the surface is rough [11]. This is not surprising in view of the transformation to a rough phase observed on the (001) -oriented Pt surface at 1820 K [10].

As the temperature is lowered below 1820 K, a peak

corresponding to the specular rod of the (001) facets develops at $H=0$ (see Fig. 2). A second peak at the buckling wave vector $H=0.2$ signals the hexagonal reconstruction of the (001) facets. Thus, 1820 K marks the onset of faceting. As the temperature is lowered further, the specular intensity of the (001) facets increases, while that of the stepped domains decreases and shifts to larger H . This implies that the area of the (001) facets grows at the expense of the stepped phase. However, in order to preserve the macroscopic surface miscut, the tilt angle must also increase.

The temperature dependence of the tilt angle α (obtained in three different experiments) is plotted in Fig. 3. Above 1820 K, the surface is oriented along the direction of the macroscopic miscut ($\alpha=1.4^\circ$). Between 1820 and 1620 K, the tilt angle increases continuously from 1.4° to 15.5° . Evidently, the variation of the tilt angle follows a one-half power law versus reduced temperature. This is shown by the solid line in Fig. 3, which represents the best fit of the data to the form $\alpha = \alpha_0 t^{\bar{\beta}}$ with the parameters: $\bar{\beta} = 0.50 \pm 0.05$, $T_0 = 1820 \pm 10$ K, and $\alpha_0 = 45^\circ \pm 5^\circ$.

In a thermodynamic context, Fig. 3 represents a temperature-orientation phase diagram for Pt surfaces near the (001) direction, and for tilt angles in the (HHL) plane. For temperatures above 1620 K, the solid line indicates the boundary between one-phase and two-phase regions. That the surface normal of the hexagonally reconstructed phase is aligned with the (001) direction suggests that the (001) direction corresponds to a cusp in the orientation dependence of the free energy for the hexagonally reconstructed phase. In this case, the exponent $\bar{\beta}$ may be directly related to the functional form of the rough-phase free energy versus orientation, $f(\alpha)$. Specifically, for $f(\alpha) = f_1|\alpha| + f_\lambda|\alpha|^\lambda$, where f_1 , f_λ , and λ are constants, it is straightforward to show that $\bar{\beta} = 1/\lambda$ and $\alpha_0 = [l/(\lambda - 1)f_\lambda]^{1/\lambda}$. l is the latent heat per unit surface area of the rough-to-hexagonal transformation of the (001)-oriented surface [3,4,6]. For a *rough* solid surface, the step-free energy is zero (i.e., $f_1 = 0$), $\lambda = 2$, and $2f_2$ is the surface stiffness [14]. It follows that $\bar{\beta} = \frac{1}{2}$, which

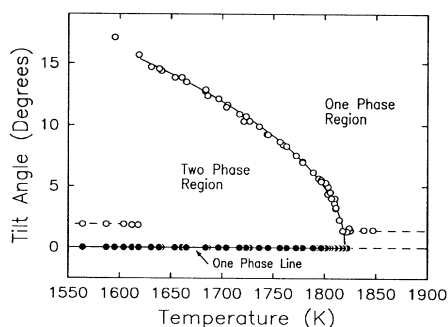


FIG. 3. Temperature dependence of the measured tilt angles on the stepped Pt(001) surface.

coincides with our experimental result. In contrast, for a *smooth* surface, it is expected that $\lambda=3$ and $\bar{\beta} = \frac{1}{3}$ [3,4,6]. Thus, the observed temperature dependence of the phase boundary supports the identification of the high-temperature phase of the Pt(001) surface and its vicinals as rough.

It is noteworthy that the phase behavior of the hexagonal reconstruction on the (001) facets closely follows that observed earlier on the (001)-oriented Pt surface [8,9]. Briefly, for temperatures between 1820 and 1680 K, we find that the principal hexagonal wave vector of the incommensurate, hexagonally reconstructed overlayer is aligned with the cubic (110) direction. As the temperature is reduced below 1680 K, there is a continuous rotational transformation in which domains of the hexagonal overlayer rotate continuously versus temperature to angles $\pm 0.9^\circ$ away from the (110) direction. A second, discontinuous rotational transformation occurs at about 1620 K, as signaled by the appearance of hexagonal domains with rotation angles of $\pm 0.8^\circ$. The buckling wave vector characteristic of hexagonal reconstructions also rotates on the continuously and discontinuously rotated domains to $\pm 5.3^\circ$ and $\pm 4.8^\circ$, respectively.

Coincident with the discontinuous rotational transformation of the (001) facets at 1620 K is a second faceting transformation. Specifically, the tilt angle of the stepped domains changes from 16° to 1.9° (see Figs. 2 and 3) and the azimuthal orientation rotates by $\pm 4.8^\circ$ away from the (110) direction. In addition, the tilted domains reconstruct at this temperature to form a buckled and rotated hexagonal structure. The rotation angles are the same as those which occur for the discontinuously rotated hexagonal domains on the (001) facets ($\pm 0.8^\circ$). Thus, below 1620 K continuously and discontinuously rotated hexagonal domains coexist on the (001) facets. For the stepped phase, only discontinuously rotated hexagonal domains are observed. Consistent with the ideas of Grey and Bohr [12], it is nevertheless remarkable that the step edges are aligned with the troughs and crests of the surface buckling of the discontinuously rotated hexagonal domains on both the stepped phase and the (001) facets. This suggests that the rotation angle of the discontinuously rotated hexagonal domains on the (001) facets may be determined by the orientation of the steps at the (001) facet borders [12], whereas the rotation angle of the continuously rotated hexagonal domains is intrinsic to the (001) facets.

These latter results are illustrated in Fig. 4, which shows scans taken along the direction of the buckling wave vector of the discontinuously rotated hexagonal domains for temperatures decreasing from 1619 to 1281 K. The scan path is shown as a solid line in the reciprocal space map shown in the inset to Fig. 4. The peaks located at $H=1.00$ and $H=1.22$ in each scan correspond to the $(H,K) = (1,1)$ bulk truncation rod and the (positively rotated) principal hexagonal rod of the (001)

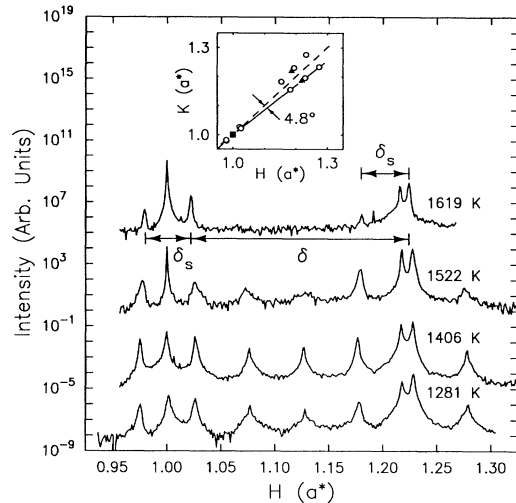


FIG. 4. High-resolution scans along the path shown as a solid line in the inset for several temperatures below 1620 K. Inset: map of the H - K plane of reciprocal space ($L=0.05$) for temperatures less than 1620 K. Solid symbols indicate rods from the (001) facets; open symbols indicate rods from the tilted domains.

facets, respectively. This assignment was made on the basis of the observed L dependence of these peaks [11]. On either side of the truncation rod of the (001) facets are two more peaks, separated by the step wave vector δ_s . They correspond to truncation rods of the tilted domains, and emanate from the (111) and (11 $\bar{1}$) bulk Bragg reflections. δ_s is inversely proportional to the terrace width and its direction is perpendicular to the steps. The peak at $H=1.23$ corresponds to the principal hexagonal rod of the reconstructed, tilted phase. It is also decorated by satellite rods of the same separation δ_s . The buckling wave vector (δ) is the difference between the principal hexagonal wave vector and the truncation rod which passes through the (11 $\bar{1}$) bulk Bragg reflection, as shown in Fig. 4. From these data, it is clear that the step wave vector δ_s is parallel to the discontinuously rotated buckling wave vector on both the stepped domains and the (001) facets.

Finally, we note that as the temperature is lowered from 1620 K, additional harmonics of the step wave vector appear and grow (see Fig. 4). While the magnitude of the buckling wave vector is approximately independent of temperature, that of the step wave vector increases from $0.058a^*$ at 1620 K to $0.067a^*$ at 1500 K, and locks to that value below 1500 K. It is striking that at 1500 K, this wave vector is precisely $\frac{1}{4}$ the buckling wave vector ($0.268a^*$). Thus, there is an incommensurate-commensurate transformation in which four periods of the surface buckling traverse each terrace between neighboring steps.

This is the first direct experimental observation of magic vicinals.

In summary, we have characterized the phase behavior of a stepped Pt(001) surface between room temperature and the bulk melting temperature. Above 1820 K, a rough surface is observed. For temperatures between 1820 and 1620 K, we find coexistence among unstepped, hexagonally reconstructed (001) facets and stepped, unreconstructed domains. The tilt angle of the stepped domains shows a one-half power-law dependence on reduced temperature. At 1620 K, there is a second morphological transformation at which the unreconstructed domains disappear to be replaced by magic vicinals. An intriguing question is whether other magic vicinals will occur when three, two, or even one buckling period fits onto each terrace. Preliminary results of recent experiments on a Pt(001) surface with a larger miscut (3°) suggest that the buckling wave vector locks to the step wave vector with a period equal to the terrace width at comparable temperatures [11].

We would like to thank G. W. Ownby for assistance in preparing the sample. Work performed at Brookhaven National Laboratory is supported by the U.S. DOE under Contract No. DE-AC0276CH00016. Work performed at Oak Ridge National Laboratory is sponsored by the Division of Material Sciences, U.S. DOE under Contract No. DE-AC05-84OR21400 with Martin Marietta Systems, Inc. Work at MIT is supported by the NSF DMR-9119675. Beamline X20A is supported by NSF DMR-9022933 and by IBM.

- [1] J. W. Cahn, *J. Phys. (Paris), Colloq.* **43**, C6-199 (1982).
- [2] A.-C. Shi and M. Wortis, *Phys. Rev. B* **37**, 7793 (1988).
- [3] R. J. Phaneuf and E. D. Williams, *Phys. Rev. Lett.* **58**, 2563 (1987).
- [4] R. Q. Hwang, E. D. Williams, and R. L. Park, *Phys. Rev. B* **40**, 11716 (1989).
- [5] P. Nozières, *J. Phys. (Paris)* **50**, 2541 (1989).
- [6] D. Y. Noh, K. I. Blum, M. J. Ramstead, and R. J. Birgeneau, *Phys. Rev. B* **44**, 10969 (1991).
- [7] A. Bartolini, F. Ercolessi, and E. Tosatti, *Phys. Rev. Lett.* **63**, 872 (1989).
- [8] D. Gibbs *et al.*, *Phys. Rev. Lett.* **67**, 3117 (1991).
- [9] D. L. Abernathy *et al.*, *Phys. Rev. B* **45**, 9272 (1992).
- [10] D. L. Abernathy *et al.*, *Phys. Rev. Lett.* **69**, 941 (1992).
- [11] M. Yoon, S. G. J. Mochrie, D. M. Zehner, G. M. Watson, and D. Gibbs (unpublished).
- [12] F. Grey and J. Bohr, *Europhys. Lett.* **18**, 717 (1992).
- [13] D. L. Abernathy, Ph.D. thesis, Massachusetts Institute of Technology, Cambridge, Massachusetts, 1993.
- [14] J. D. Weeks, in *Ordering in Strongly Fluctuating Condensed Matter Systems*, edited by T. Riste (Plenum, New York, 1980).